THE JOURNAL OF BIOLOGICAL CHEMISTRY
Vol. 278, No. 22, Issue of May 30, pp. 20185–20191, 2003

Printed in U.S.A.

Total Conversion of Bifunctional Catalase-Peroxidase (KatG) to Monofunctional Peroxidase by Exchange of a Conserved Distal Side Tyrosine*

Received for publication, November 14, 2002, and in revised form, March 18, 2003
Published, JBC Papers in Press, March 20, 2003, DOI 10.1074/jbc.M211625200

Christa Jakopitsch‡, Markus Auer‡, Anabella Ivancich§, Florian Rüker¶, Paul Georg Furtmüller‡, and Christian Obinger‡‖

From the ‡Institute of Chemistry, University of Agricultural Sciences, Muthgasse 18, A-1190 Vienna, Austria, the §Service de Bioénergétique, URA 2096 CNRS, Département de Biologie Joliot-Curie, CEA Saclay, 91191 Gif-sur-Yvette, France, and the ¶Institute of Applied Microbiology, University of Agricultural Sciences, Muthgasse 18, A-1190 Vienna, Austria

Catalase-peroxidases (KatGs) are unique peroxidases exhibiting a high catalase activity and a peroxidase activity with a wide range of artificial electron donors. Exchange of tyrosine 249 in *Synechocystis* KatG, a distal side residue found in all as yet sequenced KatGs, had dramatic consequences on the bifunctional activity and the spectral features of the redox intermediate compound II. The Y249F variant lost catalase activity but retained a peroxidase activity (substrates *o*-dianisidine, pyrogallol, guaiacol, tyrosine, and ascorbate) similar to the wild-type protein. In contrast to wild-type KatG and similar to monofunctional peroxidases, the formation of the redox intermediate compound I could be followed spectroscopically even by addition of equimolar hydrogen peroxide to ferric Y249F. The corresponding bimolecular rate constant was determined to be (1.1 ± 0.1) × 10^7 M^{-1} s^{-1} (pH 7 and 15 °C), which is typical for most peroxidases. Additionally, for the first time a clear transition of compound I to an oxoferryl-like compound II with peaks at 418, 530, and 558 nm was monitored when one-electron donors were added to compound I. Rate constants of reaction of compound I and compound II with tyrosine ((5.0 ± 0.3) × 10^4 M^{-1} s^{-1} and (1.7 ± 0.4) × 10^2 M^{-1} s^{-1}) and ascorbate ((1.3 ± 0.2) × 10^4 M^{-1} s^{-1} and (8.8 ± 0.1) × 10^1 M^{-1} s^{-1} at pH 7 and 15 °C) were determined by using the sequential stopped-flow technique. The relevance of these findings is discussed with respect to the bifunctional activity of KatGs and the recently published first crystal structure.

Catalase-peroxidases (KatGs)[1] are found in archaebacteria, eubacteria, and fungi. On the basis of sequence similarities with fungal cytochrome *c* peroxidase (CCP) and plant ascorbate peroxidases (APXs), KatGs have been shown to be members of class I of the superfamily of plant, fungal, and bacterial heme peroxidases (1). Recently, the 2.0-Å crystal structure of the KatG from the archaebacterium *Haloarcula marismortui* has been published (2). It clearly showed that in KatGs the conserved proximal amino acids His, Asp, and Trp and the conserved distal amino acids Trp, Arg, and His have coordinates very similar to CCP and APX (Fig. 1). Despite this homology, class I peroxidases differ in their reactivities toward hydrogen peroxide and one-electron donors as well as in the electronic and spectral features of their redox intermediates. These differences are shown in the generalized reaction scheme of Fig. 2. In the first phase of the catalytic cycles of heme peroxidases and catalases, the ferric enzyme is oxidized by hydrogen peroxide to the redox intermediate compound I, and a water molecule is formed (see Fig. 2, *Reaction 1*). Compound I is the key oxidizing intermediate and is two oxidizing equivalents above that of the native ferric enzyme with an oxoferryl ($Fe^{IV}=O$) center in combination with either a porphyrin π-cation radical or an amino acid radical ($R^{\bullet+}$). Ascorbate peroxidases have been shown to form a π-cation radical (3) whereas in CCP Trp-191 is the radical site (4).

The main difference in the enzymatic mechanism between catalases and peroxidases is compound I reduction. In a catalase cycle a second peroxide molecule is used as a reducing agent for compound I regenerating the native enzyme and releasing molecular oxygen (*Reaction 2*). Catalase-peroxidases have a predominant catalase activity (5–9) whereas no substantial catalase activity has ever been reported for either CCP or APX. Since with hydrogen peroxide compound I reduction (k_2) is much faster than compound I formation (k_1), even with a stopped-flow machine it is unlikely to monitor compound I formation of wild-type KatG. Thus, under steady-state turnover conditions the ferric redox state dominates (8, 10).

Recently, the role of distal Trp, Arg, and His (Fig. 1) was studied in the KatGs from *Escherichia coli* (8, 10) and from the cyanobacterium *Synechocystis* PCC 6803 (10, 11). The data presented in these articles suggest that the distal His and Arg in KatGs have a role in the heterolytic cleavage of hydrogen peroxide (*Reaction 1*) similar to other peroxidases (12). By contrast, the distal Trp has been shown to be essential for H_2O_2 oxidation, *i.e.* the two-electron reduction step of compound I back to the ferric protein (*Reaction 2*). The reasoning for this was based on the observations that in the Trp variants: (i) the catalase activity was significantly reduced (8) or even lost (10, 11), whereas (ii) the ratio of peroxidase to catalase activity was strongly increased (8, 10) indicating that compound I formation was not influenced by this mutation.

In the peroxidase reaction compound I is transformed in the first one-electron reduction to compound II containing either an oxoferryl ($Fe^{IV}=O$) center or an amino acid radical ($R^{\bullet+}$) in combination with Fe^{III} (Fig. 2, *Reaction 3*). Compound II is

* This work was supported by Austrian Science Funds (FWF project P15417). The costs of publication of this article were defrayed in part by the payment of page charges. This article must therefore be hereby marked "*advertisement*" in accordance with 18 U.S.C. Section 1734 solely to indicate this fact.

‖ To whom correspondence should be addressed. Fax: 43-1-36006-6059; E-mail: christian.obinger@boku.ac.at.

[1] The abbreviations used are: KatGs, catalase-peroxidases; APX, ascorbate peroxidase; CCP, cytochrome *c* peroxidase; HRP, horseradish peroxidase; CT1 (>600 nm), long wavelength porphyrin-to-metal charge transfer band; 5-c, five-coordinate; 6-c, six-coordinate; HS, high-spin; LS, low-spin; POA, peroxoacetic acid; EPR, electron paramagnetic resonance; CD, circular dichroism; por, porphyrin.

(A)

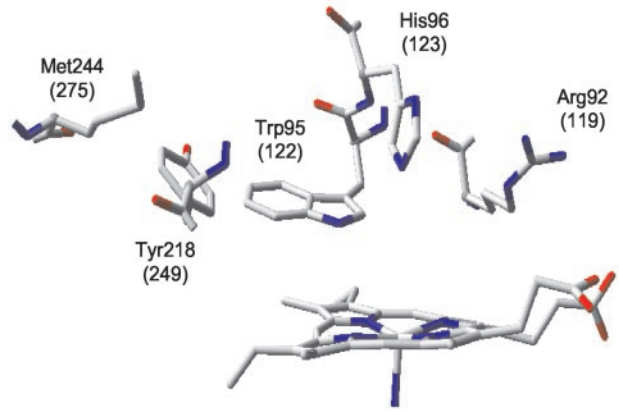

(B)

```
KatG_Syn6803 208 PEKDIYWGAEKEWLASSDHRYGSEDRESLENPLAAVQMGLIYVNPEGVDGHPDPLCTAQDVRTTF-ARMAM 277
KatG_ Halmar 181 EDKAVNWGPEDEFETQERFD----EPGEIQEGLGASVMGLIYVNPEGPDGNPDPEASAKNIRQTF-DRMAM 246
KatG_Myctub  193 PDE-VYWGKEATWLGDERY----SGKRDLENPLAAVQMGLIYVNPEGPNGNPDPMAAAVDIRETF-RRMAM 257
KatG_Esccol  191 PDLDVNWGDEKAWLT-HRHPEA-----LAKAPLGATEMGLIYVNPEGPDHSGEPLSAAAAIRATF-GNMGM 254
CCP_Saccer   136 DT-------------------------------------------TPD-NGRLPDADKDAGYVRTFF-QRLNM 163
APX_Pissat   125 PP-------------------------------------------PEGR--LPDATKGSDHLRDVFGKAMGL 151
```

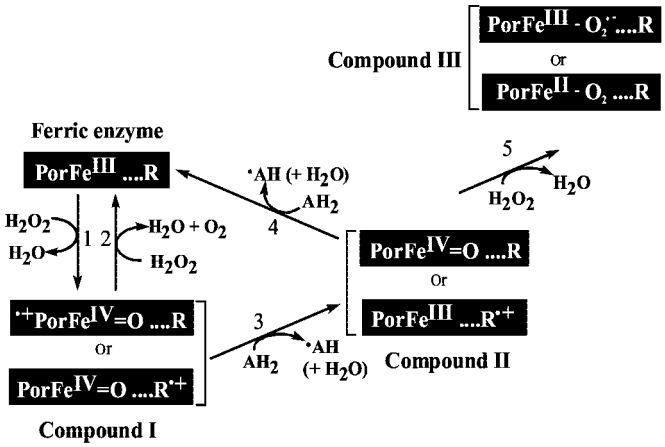

FIG. 1. **Distal side residues of catalase-peroxidase from *H. marismortui*.** *A*, distal side residues of *H. marismortui* KatG. The figure was constructed using the coordinates deposited in the Protein Data Bank (accession code 1ITK). The amino acid numbering is for *H. marismortui* KatG, but numbers in parentheses denote numbering for *Synechocystis* KatG. *B*, multiple sequence alignment performed for all three branches of class I peroxidases. KatG-typical distal tyrosine is in *blue* and distal methionine, which is found in both KatGs and APXs, is *bold*. KatG_Syn6803, catalase-peroxidase from *Synechocystis* PCC6803; KatG_Halmar, catalase-peroxidase from *H. marismortui*; KatG_Myctub, catalase-peroxidase from *M. tuberculosis*; KatG_Esccol, catalase-peroxidase from *E. coli*; CCP_Saccer, cytochrome *c* peroxidase from *Saccharomyces cerevisiae*; APX_Pissat, ascorbate peroxidase from *Pisum sativum*.

FIG. 2. **Generalized reaction scheme of peroxidases.** In the first step H_2O_2 is used for compound I formation (*Reaction 1*). Compound I is two oxidizing equivalents above that of the native enzyme with a porphyrin π−cation radical in combination with an iron(IV) center or an amino acid radical in combination with iron(IV). Compound I can react with a second H_2O_2 reducing the enzyme back to the ferric state (*Reaction 2*, catalase reaction). In the peroxidase reaction compound I is transformed in the first one-electron reduction to compound II containing either an iron(IV) center or an amino acid radical ($R^{\bullet}$) in combination with iron(III) (*Reaction 3*). Compound II is finally reduced back to ferric peroxidase in a second one-electron reduction (*Reaction 4*). Compound III (oxyperoxidase) is formed with excess H_2O_2. It exists as resonance structure with the iron(III)-superoxide form dominating (12).

finally reduced back to ferric peroxidase in a second one-electron reduction (*Reaction 4*). Both APXs and CCP cannot perform Reaction 2 and thus reduce compound I via compound II exclusively, thereby oxidizing the preferred electron donors ascorbate and cytochrome *c*, respectively. By contrast, in the catalase-peroxidases both the peroxidase (*Reactions 1*, *3*, and *4*) and the catalase cycle (*Reactions 1* and *2*) are active.

The nature of KatG compound II is unclear. In earlier stopped-flow spectroscopy studies no optical evidence for a typical (red-shifted) oxoferryl-type compound II was observed when electron donors were added to compound I formed by peroxoacetic acid. The resulting intermediate exhibited similar spectral characteristics as the ferric enzyme, which was interpreted as a species containing an oxidized amino acid ($R^{\bullet+}$) in combination with Fe^{III} (Fig. 2) (10, 13). It is of note that no EPR evidence of such intermediate has been observed and that rate constants of *Reaction 4* in KatGs are unknown so far.

The debate about the structural requirements that enable a peroxidase to catalyze H_2O_2 oxidation (*Reaction 2*) is still going on. Here, we report on the role of a distal tyrosine, which is found in all catalase-peroxidases sequenced so far, but not in CCP and APX (Fig. 1). Exchange of Tyr-249 in *Synechocystis* KatG by Phe completely transformed the catalase-peroxidase to a monofunctional peroxidase, which lost its catalase activity but fully retained its peroxidase activity. As a consequence compound I formation (Fig. 1, *Reaction 1*) could be followed by addition of equimolar H_2O_2 and the calculated rate constant is shown to be similar to plant-type peroxidases. Hydrogen peroxide oxidation by Y249F (*Reaction 2*) was negligible, but the peroxidatic cycle was fully active. For the first time a KatG compound II with an oxoferryl-type spectrum was observed allowing the determination of rate constants of both its formation (*Reaction 3*) and reduction (*Reaction 4*). The findings are compared with similar reactions of wild-type KatG and other peroxidases and are discussed with respect to the prediction of novel covalent bonds in *H. marismortui* KatG (2), which include the conserved distal tryptophan and tyrosine (Fig. 1), and the recent report about the formation of tyrosyl radical(s) in *Mycobacterium tuberculosis* KatG during reaction of the resting enzyme with alkyl peroxides (14).

MATERIALS AND METHODS

Reagents—Standard chemicals and biochemicals were obtained from Sigma Chemical Co. at the highest grade available. Expression, purification of KatGs from *Synechocystis* and spectrophotometric characterization of wild-type and mutant proteins were described previously (6, 11).

Mutagenesis—Oligonucleotide site-directed mutagenesis was performed using PCR-mediated introduction of silent mutations as described (11). A pET-3a expression vector, that contained the cloned catalase-peroxidase gene from the cyanobacterium *Synechocystis* PCC 6803 (6, 11), was used as the template for PCR. At first unique restriction sites were selected flanking the region to be mutated. The flanking primers were 5′-AAT GAT CAG GTA CCG GCC AGT AAA TG-3′ containing a *Kpn*I restriction site and 5′-AGTGCAGACTAGTTCG-GAAACG-3′ containing a *Spe*I restriction site. The following mutant primer with the desired mutation and a silent mutation introducing a restriction site were constructed (point mutations italicized and restriction sites underlined): 5′-TGGGATTAATTT*T*CGTTAA<u>TCCG</u>GAGGG-GGT GG-3′ and 5′- CACCCCC<u>TCCG</u>G*A*TTAACG*A*AAATTAATCCCA-

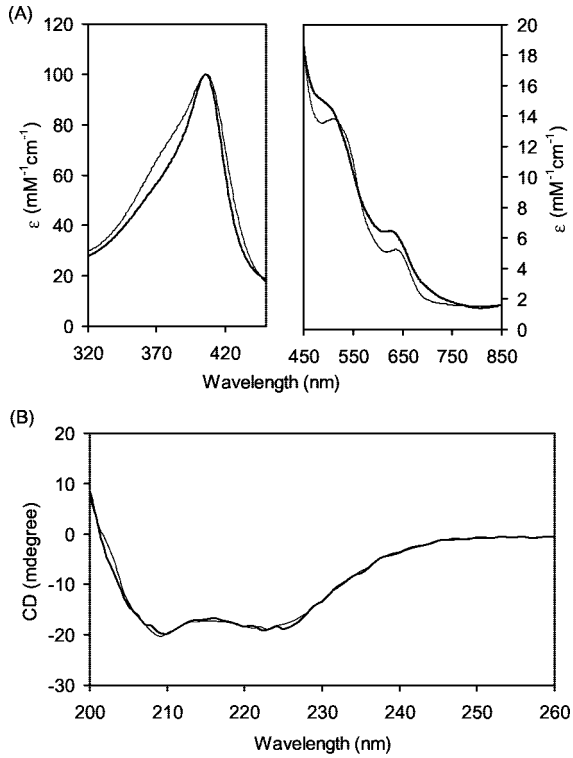

FIG. 3. **UV-Vis and circular dichroism spectra of ferric *Synechocystis* wild-type KatG and of Y249F.** *A*, UV-Vis spectra of wild-type KatG (*bold*) and Y249F. Conditions: ferric proteins in 50 mM phosphate buffer, pH 7.0 and 25 °C. The absorbance ratio (A_{Soret}/A_{280}) of the proteins was 0.60 for wild-type KatG, 0.52 for Y249F, respectively. The region between 450 and 850 nm has been expanded 6-fold. *B*, circular dichroism spectra of wild-type KatG (*bold*) and Y249F. Conditions: ferric proteins (0.15 μM) in 10 mM phosphate buffer, pH 7.0 and 25 °C.

TTTG-3′ changed Tyr-249 to Phe. The fragment defined by the *Kpn*I and *Spe*I restriction sites was replaced by the new construct containing the point mutation. The construct was sequenced to verify DNA changes using thermal cycle sequencing.

Spectroscopic Studies—Optical spectra were recorded on a diode array spectrophotometer (Zeiss Specord S10) and a Hitachi U-3000 spectrophotometer equipped with a thermostatted cell holder.

Circular dichroism studies were carried out using a JASCO J-600 spectropolarimeter. Far-UV (190−260 nm) experiments were carried out using protein concentrations of 0.15 μM, and the path length of the cuvette was 10 mm. A good signal-to-noise ratio in the CD spectra was obtained by averaging twelve scans (resolution: 1 nm; bandwidth: 1 nm; response 16 s; scan speed 20 nm/min). The protein concentration was calculated from the known amino acid composition and absorption at 280 nm according to Gill and Hippel (15).

Steady-state Kinetics—Catalase activity was determined polarographically in 50 mM phosphate buffer using a Clark-type electrode (YSI 5331 Oxygen Probe) inserted into a stirred water bath (YSI 5301B) at 30 °C. Alternatively, the catalase activity was measured by continuously monitoring hydrogen peroxide concentration polarographically with a platinum electrode covered with a hydrophilic membrane and fitted to the Amperometric Biosensor Detector 3001 (Universal Sensors, Inc.). The applied electrode potential at pH 7 was 650 mV, and the H_2O_2 electrode filling solution was prepared freshly half daily. The electrode was calibrated against known concentrations of hydrogen peroxide. All reactions were performed at 30 °C and started by the addition of KatG. One unit of catalase is defined as the amount that decomposes 1 μmol of H_2O_2/min at pH 7 and 30 °C.

Peroxidase activity was monitored spectrophotometrically using 1 mM H_2O_2 (or 1 mM peroxoacetic acid) and 5 mM guaiacol (ϵ_{470} = 26.6 mM^{-1} cm^{-1}) or 1 mM *o*-dianisidine (ϵ_{460} = 11.3 mM^{-1} cm^{-1}) or 1 mM tyrosine (ϵ_{315} = 3.6 mM^{-1} cm^{-1}) or 1 mM ascorbate (ϵ_{290} = 2.8 $mM^{-1}cm^{-1}$). Peroxidase activity with pyrogallol was monitored using 100 μM H_2O_2 and 20 mM pyrogallol (ϵ_{430} = 2.47 mM^{-1} cm^{-1}). One unit of peroxidase is defined as the amount that decomposes 1 μmol of electron donor/min at pH 7 and 30 °C. Steady-state spectrophotometric measurements were made on a diode-array spectrophotometer Specord S10 (Zeiss) and a Hitachi Model U-3000 spectrophotometer, respectively.

Transient State Kinetics—Transient state measurements were made using the model SX-18MV stopped-flow spectrophotometer from Applied Photophysics equipped with a 1-cm observation cell thermostatted at 15 °C. Calculation of pseudo first-order rate constants (k_{obs}) from experimental traces at the Soret maximum was performed with the SpectraKinetic work station v4.38 interfaced to the instrument.

The kinetics of oxidation of ferric KatG to compound I by hydrogen peroxide and peroxoacetic acid (POA) was followed in the single mixing mode at 407 nm. Ferric KatG and the peroxide were mixed to give a final concentration of 1 μM enzyme and 1–20 μM H_2O_2 or 5–35 μM peroxoacetic acid. The first data point was recorded 1.5 ms after mixing, and 2000 data points were accumulated. Second-order rate constants were calculated from the slope of the linear plot of pseudo first-order rate constants *versus* substrate concentration.

Sequential-mixing stopped-flow analysis was used to measure compound I reduction by one-electron donors. In the first step the enzyme was mixed with equimolar H_2O_2 and, after a delay time of 100 ms where compound I was built, the intermediate was mixed with the electron donors ascorbate and tyrosine. The kinetics of compound II formation was monitored at 418 nm, the wavelength of maximum absorbance of Y249F compound II. The kinetic traces were fitted using the single exponential equation of the Applied Photophysics software and, from the slopes of the linear plots of the k_{obs} values *versus* substrate concentration, the apparent second-order rate constants were obtained by linear square regression analysis.

Reduction of Y249F compound II by tyrosine or ascorbate was monitored by using the following procedures. The ferric protein (4 μM) was premixed with equimolar concentration of hydrogen peroxide in 100 mM phosphate buffer (pH 7.0). After a delay time of 10 s, the formed compound II was allowed to react with varying concentrations of reducing substrates in the same buffer. The reactions were followed at 418 nm (disappearance of compound II) or at 407 nm (formation of the ferric KatG). Alternatively, 4 μM ferric KatG was premixed with equimolar concentration of hydrogen peroxide and after a delay time of 100 ms, compound I was allowed to react with varying concentrations of reducing substrates in the same buffer. The reactions were once again measured at 418 nm. The resulting biphasic curves showed the initial formation of compound II and then its subsequent reaction with ascorbate or tyrosine causing an exponential decrease in absorbance.

All reactions were also investigated using the diode-array detector (Applied Photophysics PD.1) attached to the stopped-flow machine and the XScan Diode Array Scanning v1.07 software. Typically, in these experiments the KatG concentration was higher (*e.g.* 5 μM in the optical cell). Normal spectral data sets were also analyzed using the Pro-K simulation program from Applied Photophysics, which allows the synthesis of artificial sets of time dependent spectra as well as spectral analysis of enzyme intermediates.

EPR Spectroscopy—Conventional 9-GHz EPR measurements were performed using a Bruker ER 300 spectrometer with a standard TE_{102} cavity equipped with a liquid helium cryostat (Oxford Instrument) and a microwave frequency counter (Hewlett Packard 5350B). Typically, the compound I samples were prepared by mixing manually 2.0 mM native enzyme (100 mM Tris/maleate buffer, pH 8.0) with an excess (10-fold) of peroxoacetic acid, directly in the 4-mm EPR tubes kept at 0 °C. The reaction was stopped by rapid immersion of the EPR tube in liquid nitrogen after 10 s.

RESULTS AND DISCUSSION

Sequence analysis of all as yet published *katG* genes as well as inspection of the recently published three-dimensional structure of *H. marismortui* KatG shows the existence of a conserved distal side tyrosine (Fig. 1). Based on the observation of continuous electron densities in the x-ray structure it was suggested that this tyrosine is covalently bonded to adjacent tryptophan and methionine (2). In detail, bonds between Cϵ1 of Tyr-218 (*Haloarcula* numbering) and Cϵ2 of distal Trp-95 as well as between Cϵ2 of Tyr-218 and Sδ of Met-244 were suggested, though tryptic digestion and mass spectrometry of the reaction products were unable to prove definitely the existence of these covalent bonds in *Haloarcula* KatG. Neither in CCP nor in APXs this distal tyrosine is found, whereas the distal methionine is found in all KatGs and APXs but not in CCP (Fig. 1*B*).

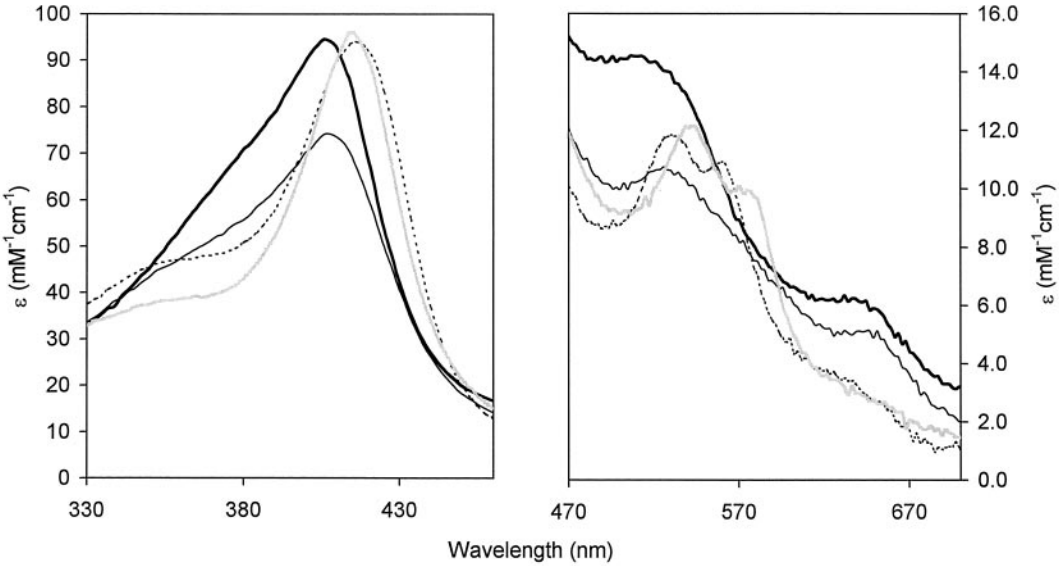

FIG. 4. **Optical absorbance spectra of the redox intermediates of the catalase-peroxidase variant Y249F.** Conditions: 50 mM phosphate buffer, pH 7.0 and 15 °C. *Bold line*, 5 μM ferric enzyme; *black line*, 5 μM compound I (formed in the stopped-flow machine by mixing the protein with equimolar H_2O_2 and taking the spectrum after 70 ms); *dotted line*, 5 μM compound II (formed in the sequential mixing mode by adding 1 mM ascorbate to compound I and taking the spectrum at 500 ms); *gray line*, 5 μM compound III (formed by mixing of the ferric protein with 100 μM H_2O_2 and taking the spectrum after 10 s).

Fig. 3 depicts the UV-Vis and CD spectra of wild-type KatG and the variant Y249F investigated in this study. In the electronic absorption spectrum of ferric wild-type KatG, both the Soret and the CT1 band (637 nm) suggest the presence of a 5-c HS heme coexisting with a 6-c HS heme (16). In Y249F the shoulder at about 380 nm increases in intensity and the CT1 band red-shifts indicating an increase of the 5-c HS heme at the expense of 6-c HS heme.

The A_{406}/A_{280} ratios (*i.e.* Reinheitszahl) of Y249F varied between 0.49 and 0.52 compared with 0.57 and 0.61 of the wild-type protein. Thus, the Reinheitszahl of Y249F was comparable to that of other KatG variants produced so far (10, 11, 13). The protein yield was 50–80 mg of recombinant KatG from 1 liter of *E. coli* culture for both wild type and Y249F.

The CD spectra of wild-type KatG and Y249F (Fig. 3*B*) are characteristic of a protein composed primarily of α-helices. Very little difference was observed between wild-type KatG and the variant. If conformational changes did occur, they must have been very localized and thus undetectable by CD experiments.

Catalase and Peroxidase Activity—Recombinant wild-type KatG exhibits an overwhelming catalase activity. The polarographically measured specific catalase activity in the presence of 5 mM hydrogen peroxide is (1160 ± 55) units/mg of protein. For wild-type *Synechocystis* KatG a turnover number (k_{cat}) of 3500 s^{-1} and a k_{cat}/K_m rate of 8.5 × 10^5 M^{-1} s^{-1} was determined which underscores the singular status KatGs have among the heme peroxidase superfamily. However, exchange of Tyr-249 led to an almost complete loss of catalase activity. With a calculated turnover number of (6 ± 3) s^{-1} more than 99.8% of wild-type catalase activity was lost, and the remaining catalase activity was now similar to that determined for various horseradish peroxidase isoenzymes (2–13) s^{-1} (17).

Most interesting was the finding that upon addition of micromolar hydrogen peroxide (1–5 μM) to 1 μM ferric Y249F KatG a red-shift in the absorbance spectrum was observed in a conventional spectrophotometer (Fig. 4). The resulting absorption bands at 418, 530, and 558 nm suggested the formation of a redox intermediate with spectral features similar to that of an oxoferryl-like compound II (12). By contrast, in wild-type KatG the dominating redox intermediate spectrum during H_2O_2 degradation (10–1000 μM) has spectral features very similar to that of the ferric enzyme (8–11).

Addition of higher concentrations of H_2O_2 (>10 μM) to ferric Y249F KatG led to the formation of an oxyferrous-like (compound III) intermediate (12), as indicated by the appearance of absorption bands at 414, 542, and 576 nm (Fig. 4). A comparable transition of native wild-type *Mycobacterium* KatG to compound III has been reported (9), but in these experiments very high concentrations (0.4 M) of hydrogen peroxide had to be added in order to produce a compound III spectrum with peaks at 418, 545, and 580 nm (9).

In the presence of peroxidase substrates the dominating redox intermediate had spectral features typical for an oxoferryl-type compound II (418, 530, and 558 nm). This has never been observed with both wild-type KatGs and mutants produced so far. However, the effect of mutation on the overall peroxidase activity was small. Both the hierarchy of substrates (pyrogallol > *o*-dianisidine > guaiacol ≫ tyrosine > ascorbate) and the determined specific peroxidase avitivities of Y249F and wild-type KatG were similar. Using hydrogen peroxide and *o*-dianisidine the specific peroxidase activities were determined to be (3.4 ± 0.3) units per mg (wild-type) and (4.1 ± 0.4) units per mg (Y249F). The corresponding activities with pyrogallol were (6.5 ± 0.4) units per mg (wild-type) and (5.5 ± 0.5) units per mg (Y249F) and with guaiacol (0.6 ± 0.2) units per mg (wild-type) and (1.2 ± 0.1) units per mg (Y249F), respectively. The pH dependence of the peroxidase activity was similar in wild-type and Y249F showing a clear maximum at pH 5.5 (not shown). The overall peroxidase activity using ascorbate and tyrosine as substrates was negligible.

Under the assumption that the redox intermediate compound I is part of both the catalase and peroxidase cycle (Fig. 2) these data suggest some loss in the peroxidase activity upon exchange of Tyr-249 by Phe, because in wild-type KatG an overwhelming catalase activity strongly favors H_2O_2 oxidation (Fig. 2, *Reaction 2*) above oxidation of one-electron donors (Fig. 2, *Reactions 3* and *4*). Using peroxoacetic acid instead of H_2O_2 simplifies the comparison of peroxidase activity of wild-type KatG and Y249F, since *Reaction 2* is negligible. In wild-type KatG the specific peroxidase activity with guaiacol as donor was about 5-times higher ((2.8 ± 0.3) units per mg) when

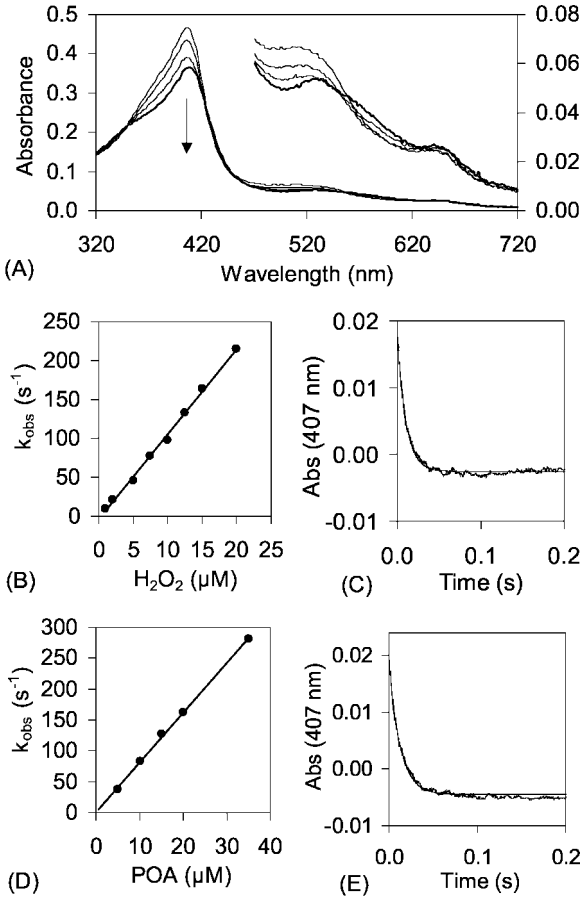

FIG. 5. **Compound I formation of the *Synechocystis* KatG variant Y249F.** *A*, spectral changes upon addition of hydrogen peroxide to ferric Y249F. Final concentrations: 5 μM H_2O_2 and 5 μM Y249F. First spectrum is that of ferric enzyme. Following spectra were taken after 6, 26, and 100 ms (*bold*), respectively. Conditions: 50 mM phosphate buffer, pH 7.0 and 15 °C. *B*, pseudo first-order rate constants for the formation of Y249F compound I plotted against hydrogen peroxide concentration. *C*, typical time trace and fit of the reaction between 1 μM Y249F and 10 μM H_2O_2 followed at 407 nm. Conditions as in *A*. *D*, pseudo first-order rate constants for the formation of Y249F compound I plotted against peroxoacetic acid (*POA*) concentration. *E*, typical time trace and fit of the reaction between 1 μM Y249F and 10 μM peroxoacetic acid followed at 407 nm. Conditions as in *A*.

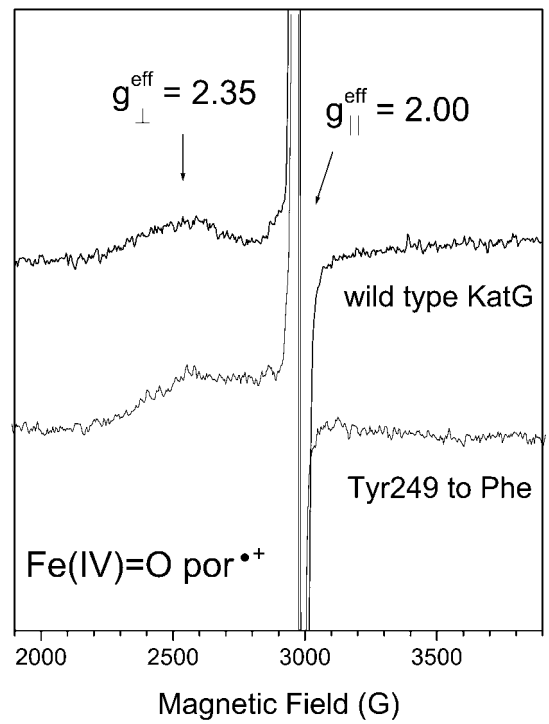

FIG. 6. **9-GHz EPR spectra of the compound I [Fe(IV)=O por$^{\cdot+}$] intermediate in wild-type and the Y249F variant of *Synechocystis* PCC 6803 catalase-peroxidase.** The broad axial spectrum with effective g-values of 2.35 and 2.00 for $g_{\perp}$ and $g_{||}$, respectively is the exchange-coupled oxoferryl-porphyrin π-cation radical [Fe(IV)=O Por$^{\cdot+}$] species. The narrow feature overlapping at g = 2.00 is a protein-based radical and has been clipped for clarity. Experimental conditions: temperature, 4.2 K; modulation amplitude, 3.5 G; modulation frequency, 100 kHz; microwave power, 1 milliwatt.

peroxoacetic acid was used instead of H_2O_2. Under identical conditions the activity of the variant Y249F was ((1.5 ± 0.2) units per mg), which is about 46% lower compared with wild-type activity.

Compound I Formation—Compound I is normally a difficult species to identify in catalase-peroxidases because of the potential for rapid reduction by H_2O_2 in the catalase cycle. Only by use of organic peroxides (*e.g.* peroxoacetic acid) a compound I spectrum can be obtained that is distinguished from the resting state by a 40–45% hypochromicity, and its formation can be followed as exponential absorbance decrease at the Soret maximum. However, exchange of Tyr-249 allowed to follow compound I formation even with equimolar hydrogen peroxide. In Fig. 5*A* the spectral changes are shown when 5 μM ferric KatG reacted with 5 μM H_2O_2. A decrease in the Soret band (hypochromicity, 27%) was observed with two isosbestic points at 351 and 431 nm. The reaction was monophasic (Fig. 5*C*) indicating pseudo first-order kinetics. The plot of the first-order rate constants, k_{obs}, *versus* H_2O_2 concentration was linear and from the slope a bimolecular rate constant was determined to be (1.1 ± 0.3) × 10^7 M^{-1} s^{-1} at 15 °C and pH 7.0 (Fig. 5*B*). The rate of compound I formation of pea cytosolic APX was reported to be 8.3 × 10^7 M^{-1} s^{-1} (18) or 4.0 × 10^7 M^{-1} s^{-1} (19) and the rates of CCP and other heme peroxidases were shown to be in the range of 10^7 to 10^8 M^{-1} s^{-1} (12, 20–22). Thus, the kinetics of Tyr-249 compound I formation is typical for heme peroxidases and suggests that formation of KatG compound I follows the Poulos and Kraut mechanism involving the peroxidase-typical distal histidine and arginine residues (23). This is underscored by the recent findings that exchange of the distal histidine or arginine in KatGs strongly effects compound I formation and thus both the overall catalase and the peroxidase activity (8, 11). By using peroxoacetic acid to oxidize ferric Y249F KatG identical spectral changes and kinetics were obtained (Fig. 5*E*). The bimolecular rate constant was determined to be (8.0 ± 0.3) × 10^6 M^{-1} s^{-1} at 15 °C and pH 7.0 (Fig. 5*D*).

EPR Spectrum of Compound I—Fig. 6 shows the 9 GHz-EPR spectra of the intermediate(s) obtained by the reaction of ferric catalase-peroxidase with peroxoacetic acid. A broad axial signal extending over about 2000 *G* was observed for both the wild-type enzyme and the Y249F variant. The axial pattern with effective g-values of $g_{\perp}$ = 2.35 and $g_{||}$ = 2.00 for the wild-type enzyme was consistent with the typical compound I intermediate, the [Fe^{IV}=O Por$^{\cdot+}$] species, well characterized for catalases and peroxidases (3, 24–26). Close inspection of the [Fe^{IV}=O Por$^{\cdot+}$] EPR spectra of the Y249F KatG variant showed differences in the overall shape as compared with the wild-type spectrum, in particular the low-field edge ($g_{\perp}$ component) that shifted upfield. Similar, although more dramatic, effects were induced by pH changes in the turnip peroxidase compound I spectrum and were interpreted as the protein fine-tuning effect on the nature of the magnetic interaction of the oxoferryl-porphyrin radical pair (26). In the case of *Synechocystis* KatG, the spectral differences between wild-type and the Y249F var-

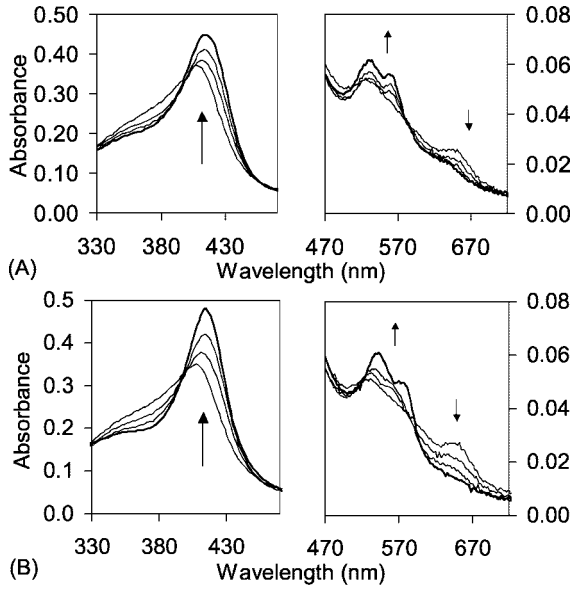

FIG. 7. **Compound I decay to compound II and formation of compound III.** *A*, spectral changes upon addition of hydrogen peroxide to ferric Y249F. Final concentrations: 5 μM H_2O_2 and 5 μM Y249F. First spectrum is that of compound I taken at 70 ms. Following spectra were taken after 500 ms, 1.2 s and 10 s (*bold*, peaks at 418, 530, and 558 nm, respectively). Conditions: 50 mM phosphate buffer, pH 7.0 and 15 °C. *B*, spectral changes upon addition of hydrogen peroxide to ferric Y249F. Final concentrations: 50 μM H_2O_2 and 5 μM Y249F. First spectrum is taken at 6 ms, following spectra at 400 ms, 1.5 s and 10 s (*bold*, peaks at 414, 542, and 576 nm, respectively). Conditions: 50 mM phosphate buffer, pH 7.0 and 15 °C.

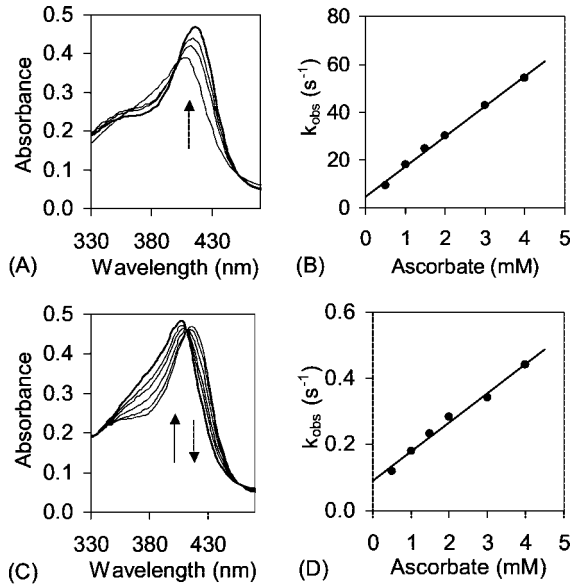

FIG. 8. **Formation and reduction of compound II of the *Synechocystis* KatG variant Y249F.** *A*, spectral changes upon addition of ascorbate to Y249F compound I formed with equimolar hydrogen peroxide. Final concentrations: 1 μM Y249F compound I and 2.5 mM ascorbate. First spectrum is that of compound I formed after 70 ms (*i.e.* delay time). Second spectrum was taken 10 ms after ascorbate was mixed with compound I. Following spectra were taken at 20 ms and 100 ms (*bold*) respectively. Conditions: 50 mM phosphate buffer, pH 7.0 and 15 °C. *B*, pseudo first-order rate constants for Y249F compound I reduction plotted against ascorbate concentration. *C*, spectral changes upon addition of ascorbate to Y249F compound II. Final concentrations: 1 μM Y249F compound II and 2.5 mM ascorbate. First spectrum is that of compound II formed 160 ms after compound I was mixed with ascorbate. Following spectra were taken at 1.2 s, 1.8 s, 3.8 s and 7 s (*bold*), respectively. Conditions: 50 mM phosphate buffer, pH 7.0 and 15 °C. *D*, pseudo first-order rate constants for Y249F compound II reduction plotted against ascorbate concentration.

iant may reflect subtle structural changes in the heme environment induced by the mutation, that were not detected by the CD experiments.

It is of note that the magnetic interaction (ferromagnetic exchange coupling) between the porphyrin π-cation radical ($Por^{\bullet+}$) and the oxoferryl (Fe(IV)=O) moiety is at the origin of the broad and axial EPR spectrum for the compound I intermediate (27). Accordingly, the previously reported EPR spectrum of the compound I intermediate in *E. coli* HPI catalase-peroxidase (8) would be consistent with the $g_{\|} = 2$ component of the broad signal. In the *Synechocystis* catalase-peroxidase EPR spectrum (see Fig. 6), a much narrower radical signal (overall width of 20 *G*, effective $g_{iso} = 2.0043$) overlapped with the $g_{\|}$ component of the broad oxoferryl-porphyrin radical spectrum. A similar narrow signal has been recently reported for *M. tuberculosis* catalase-peroxidase and assigned to a tyrosyl radical intermediate (14).

Taken together, the features of the UV-VIS spectrum of the peroxoacetic-acid induced intermediate in the Y249F variant (Fig. 5) and the broad EPR signal (Fig. 6) are totally consistent with the formation of the oxoferryl-porphyrin radical intermediate.

Compound I Decay—As indicated above Y249F compound I was not stable. At pH 7.0 and in the absence of an external electron donor it decayed to an intermediate with spectral features reminescent of a classical oxoferryl-type compound II (Fig. 7*A*). The rate of decay was slow (0.6 ± 0.1) s^{-1}, and the absorbance increase at 418 nm reached a plateau after 8 s.

Fig. 7*B* shows what happened when H_2O_2 at concentrations higher than 10 μM was mixed with 1 μM ferric Y249F KatG. An intermediate with spectral features different from compound II was formed. With 50 μM H_2O_2 and 5 μM Y249F the spectral transition is finished within 7 s leading to a Soret absorbance at 414 nm and two peaks at 542 and 576 nm. This is reminescent of an oxyferrous-type peroxidase intermediate, also called compound III or oxyperoxidase, and suggests a similar route of formation as in plant-type peroxidases, where it has been shown to be obtained from compound II in presence of excess hydrogen peroxide according to *Reaction 5* in Fig. 2 (12, 28). Compound III exists as a resonance structure with the ferric ion-superoxide form dominating (12) and is outside of both the catalase and peroxidase cycle.

Compound II Formation and Reduction—In the presence of a good electron donor the spontaneous decay of compound I is negligible. Fig. 8*A* shows the spectral transition when preformed Y249F compound I (5 μM) was mixed with 2.5 mM ascorbate at pH 7.0 and 15 °C. A direct transition of compound I to an oxoferryl-type (Fe^{IV}=O) compound II was seen with peaks at 418, 530, and 558 nm. Compound II formation depended strongly on the concentration of ascorbate or tyrosine. Compound II was formed (increase of absorbance at 418 nm) and, finally, reduced (decrease at 418 nm) indicating that these substrates function as electron donors for both Y249F redox intermediates. Fig. 8*A* shows the spectral transition of compound I to compound II with clear isosbestic points at 401 and 453 nm. The reaction was monitored at 418 nm, and the time traces displayed a single exponential character (not shown). From a plot of the pseudo first-order rate constants, k_{obs}, against ascorbate concentration (Fig. 8*B*), the apparent second-order rate constant (k_3) was obtained to be (1.3 ± 0.2) × 10^4 M^{-1} s^{-1} at pH 7.0 and 15 °C. Using tyrosine as donor a bimolecular rate constant of (5.0 ± 0.3) × 10^4 M^{-1} s^{-1} was calculated. The plots had finite intercepts (*e.g.* 4.6 s^{-1} in case of ascorbate) showing the existence of side reactions like the spontaneous decay of compound I to compound II as well as of subsequent

compound II reduction by the same donors. Thus, in contrast to wild-type KatG, Y249F behaves like horseradish peroxidase (12) or APX (19) and compound I reduction by a one-electron donor can be represented by *Reaction 3* in Fig. 2.

Compound II reduction was followed by mixing preformed compound I with either ascorbate or tyrosine and observing both the initial formation and reduction of compound II at 418 nm. The resulting curves were biphasic and from the exponential curve fit, k_{obs} values for compound II reduction by either ascorbate or tyrosine were obtained from the second part (*i.e.* exponential decrease at 418 nm) of the curve. The bimolecular rate constants (k_4) calculated by this method were $(8.8 \pm 0.1) \times 10^1$ M^{-1} s^{-1} for ascorbate (Fig. 8*D*) and $(1.7 \pm 0.4) \times 10^2$ M^{-1} s^{-1} for tyrosine (pH 7.0 and 15 °C). Independent of the donor, the spectral transition from compound II to ferric Y249F was direct with clear isosbestic points at 336, 412, and 457 nm, respectively (Fig. 8*C*). *Reaction 4* in Fig. 2 represents reduction of Y249F compound II.

It is interesting to note that not only the spectral features of compounds I and II of Y249F were similar to those of horseradish peroxidase (HRP), but also the reactivity was comparable. Rates of reduction of HRP compound I and II by tyrosine were determined to be 5×10^4 M^{-1} s^{-1} and 1.1×10^3 M^{-1} s^{-1} (29).

Conclusion—Wild-type KatG does not allow to follow compound I formation by H_2O_2 because of its intrinsic high catalase activity. The rate of H_2O_2 oxidation (k_2) exceeds that of H_2O_2 reduction (k_1) and the spectrum of the ferric form dominates during hydrogen peroxide degradation ($k_2 > k_1$). By contrast, upon exchange of Tyr-249 to Phe the ability of the variant to oxidize hydrogen peroxide (Fig. 2, *Reaction 2*) was substantially reduced, whereas reduction of H_2O_2 by the ferric enzyme was uneffected (Fig. 2, *Reaction 1*). As a consequence of $k_1 \gg k_2$ in Y249F, the kinetics of compound I formation resembled that of typical peroxidases as did the determined value of k_1, $(1.1 \pm 0.3) \times 10^7$ M^{-1} s^{-1} at 15 °C and pH 7.0.

Most interesting was the finding that the peroxidase cycle of Y249F was still active and followed the conventional scheme of typical plant-type peroxidases. A red-shifted oxoferryl-type compound II accumulated during the peroxidatic reaction, indicating that its reduction to the ferric enzyme (Fig. 2, *Reaction 4*) was the rate-limiting step in the cycle. This was confirmed by the stopped-flow investigations, since the distinct spectral features of Y249F allowed to determine the bimolecular rate constants of both its formation (k_3) and reduction (k_4) in the sequential stopped-flow mode. Both the ratio ($k_3 > k_4$) and the values of k_3 and k_4 were comparable to typical plant-type peroxidases.

There remains the question of why upon exchange of Tyr-249 by Phe: (i) the variant becomes incompetent in H_2O_2 oxidation (*Reaction 2*) and thus is converted from a bifunctional KatG to a monofunctional peroxidase, and (ii) a clear oxoferryl-type compound II is formed in the peroxidase cycle, which was never observed so far in the study of wild-type and mutant catalase-peroxidases. Two recently reported facts could help to design experiments to understand the dramatic catalytic consequences of this single amino acid exchange. First, EPR evidence for the formation of tyrosyl radical(s) in high yield in *M. tuberculosis* KatG during reaction of the resting enzyme with alkyl peroxides suggest a role of a tyrosyl radical in either the peroxidase or catalase pathways or in both (14). As the generalized scheme in Fig. 2 shows, protein radicals could contribute to the structure of both compound I and compound II and thus participate in both the peroxidase and catalase cycle. Based on the impossibility to observe a red-shifted compound II in the absorption spectrum of wild-type KatG, the existence of such a protein radical site in KatG compound II has been proposed (5, 10, 11, 13). Interestingly, the EPR spectrum of both the wild-type and the Y249F variant showed the presence of a protein-based radical together with the oxoferryl-porphyrin radical species. In order to test if Tyr-249 in *Synechocystis* KatG is a candidate needs further detailed investigations combining multifrequency EPR and deuterium-labeling experiments on Y249F KatG. Secondly, if considering that Trp-122 is essential for the two-electron reduction of KatG compound I by hydrogen peroxide (8, 10) and the presence of a covalent bond between Trp-122 and Tyr-249 (2), the exchange of Tyr-249 could presumably modify the coordinates of the distal Trp-122 and disturb the hydrogen-bond network on the distal side (16). It is of note that the H-bond network was shown to be necessary for the catalase pathway of the enzyme (16). However, the proposed covalent link is questionable since it could not be proven by tryptic digestion and mass spectrometry (2).

Acknowledgments—The COST Action D21 "Natural, Engineered peroxidases and synthetic model compounds with peroxidase-like activity" is thanked for supporting exchange among the laboratories.

REFERENCES

1. Welinder, K. G. (1992) *Curr. Opin. Struct. Biol.* **2,** 388–393
2. Yamada, Y., Fujiwara, T., Sato, T., Igarashi, N., and Tanaka, N. (2002) *Nat. Struct. Biol.* **9,** 691–695
3. Patterson, W. R., Poulos, T. L., and Goodin, D. B. (1995) *Biochemistry* **34,** 4342–4345
4. Sivaraja, M., Goodin, D. B., Mauk, A. G., Smith, M., and Hoffman, B. A. (1989) *Science* **245,** 738–740
5. Obinger, C., Regelsberger, G., Strasser, G., Burner, U., and Peschek, G. A. (1997) *Biochem. Biophys. Res. Commun.* **235,** 545–552
6. Jakopitsch, C., Rüker, F., Regelsberger, G., Dockal, M., Peschek, G. A., and Obinger, C. (1999) *Biol. Chem.* **380,** 1087–1096
7. Engleder, M., Regelsberger, G., Jakopitsch, C., Furtmüller, P. G., Rüker, F., Peschek, G. A., and Obinger, C. (2000) *Biochimie (Paris)* **82,** 211–219
8. Hillar, A., Peters, B., Pauls, R., Loboda, A., Zhang, H., Mauk, A. G., and Loewen, P. C. (2000) *Biochemistry* **39,** 5868–5875
9. Chouchane, S., Lippai, I., and Magliozzo, R. S. (2000) *Biochemistry* **39,** 9975–9983
10. Regelsberger, G., Jakopitsch, C., Furtmüller, P. G., Rüker, F., Switala, J., Loewen, P. C., and Obinger, C. (2001) *Biochem. Soc. Trans.* **29,** 99–105
11. Regelsberger, G., Jakopitsch, C., Rüker, F., Krois, D., Peschek, G. A., and Obinger, C. (2000) *J. Biol. Chem.* **275,** 22854–22861
12. Dunford, H. B. (1999) *Heme Peroxidases*, Wiley-VCH, New York
13. Jakopitsch, C., Regelsberger, G., Furtmüller, P. G., Rüker, F., Peschek, G. A., and Obinger, C. (2002) *J. Inorg. Biochem.* **91,** 78–86
14. Chouchane, S., Girotto, S., Yu, S., and Magliozzo, R. S. (2002) *J. Biol. Chem.* **277,** 42633–42638
15. Gill, S. C., and von Hippel, P. H. (1989) *Anal. Biochem.* **182,** 319–326
16. Heering, H. A., Indiani, C., Regelsberger, G., Jakopitsch, C., Obinger, C., and Smulevich, G. (2002) *Biochemistry* **41,** 9237–9247
17. Hiner, A. N. P., Hernandez-Ruiz, J., Garcia-Canovas, F., Smith, A. T., Arnao, M. B., and Acosta, M. (1995) *Eur. J. Biochem.* **234,** 506–512
18. Mandelman, D., Jamal, J., and Poulos, T. L. (1998) *Biochemistry* **37,** 17610–17617
19. Marquez, L. A., Quitoriano, M., Zilinskas, B. A., and Dunford, H. B. (1996) *FEBS Lett.* **389,** 153–156
20. Balny, C., Anni, H., and Yonetani, T. (1987) *FEBS Lett.* **221,** 349–354
21. Loo, S., and Erman, J. E. (1975) *Biochemistry* **14,** 3467–3470
22. Ohlsson, P. I., Yonetani, T., and Wold, S. (1986) *Biochim. Biophys. Acta* **874,** 160–166
23. Poulos, T. L., and Kraut, J. (1980) *J. Biol. Chem.* **255,** 8199–8205
24. Benecky, M. J., Frew, J. E., Scowen, N., Jones, P., Hoffman, B. M. (1993) *Biochemistry* **32,** 11929–11933
25. Ivancich, A., Jouve, H. M., Sartor, B., Gaillard, J. (1997) *Biochemistry* **36,** 9356–9364
26. Ivancich, A., Mazza, G., Desbois, A. (2001) *Biochemistry* **40,** 6860–6866
27. Schulz, C. E., Devaney, P. W., Wrinkler, H., Debrunner, P. G., Doan, N., Chiang, R., Rutter, R., Hager, L. P. (1979) *FEBS Lett.* **103,** 102–105
28. Nakajima, R., and Yamazaki, I. (1987) *J. Biol. Chem.* **262,** 2576–2581
29. Ralston, I., and Dunford, H. B. (1978) *Can. J. Biochem.* **56,** 1115–1119

Total Conversion of Bifunctional Catalase-Peroxidase (KatG) to Monofunctional Peroxidase by Exchange of a Conserved Distal Side Tyrosine

Christa Jakopitsch, Markus Auer, Anabella Ivancich, Florian Rüker, Paul Georg Furtmüller and Christian Obinger

J. Biol. Chem. 2003, 278:20185-20191.
doi: 10.1074/jbc.M211625200 originally published online March 20, 2003
